

# Flowing Characteristics of Cold Arc Jet Plasma along Open Field Lines

Kazuyuki YOSHIDA<sup>1</sup>, Tomohiko SHIBATA<sup>1</sup>, Atsushi NEZU<sup>2</sup>,  
Haruaki MATSUURA<sup>2</sup> and Hiroshi AKATSUKA<sup>1,2</sup>

<sup>1</sup>*Department of Energy Sciences, Tokyo Tech., 2-12-1-N1-10 O-Okayama Meguro-ku, Tokyo 152-8550, Japan*

<sup>2</sup>*Research Lab. Nuclear Reactors, Tokyo Tech., 2-12-1-N1-10 O-Okayama Meguro-ku, Tokyo 152-8550, Japan*

(Received: 2 September 2008 / Accepted: 17 December 2008)

We experimentally study plasma parameters including the ion acoustic Mach number and the flow direction of expanding helium plasma jet flowing along open field lines. It is experimentally found that the ion Mach number increases. We discuss the mechanism of the ion acceleration. First, since the ions do not rotate in electromagnets, the Hall and the swirl acceleration do not occur. Next, the direction of the ion flow is compared with the magnetic field. It is found that the direction of the ion flow corresponds to that of the magnetic field. Then, it is also experimentally confirmed that the plasma potential decreases at each radial position. Finally, we investigate the experimental results based on quasi one-dimensional flow model including the aerodynamic effect and the electric field. Our model describes the ion acceleration and the axial profiles of the potential drop. Consequently, it is concluded that the helium ions are accelerated both by the electric field and by the increasing cross sectional area of the flowing channel, which is determined by the magnetic flux conservation.

Keywords: open field lines, arc jet plasma, ion acceleration, Mach probe, quasi one-dimensional flow model.

## 1. Introduction

Plasma expansion along open field lines has applications and related researches, such as material processing, space propulsion and nuclear fusion. For material processing, an arc jet plasma is used for a spray coatings [1] and an ion implantation [2]. Open field lines are expected to control arc jet plasma characteristics precisely. Plasma acceleration along open field lines has potential to improve efficiency of electric propulsion for spacecrafts.

Plasma acceleration along open field lines has been studied in various types of plasmas such as an arc jet plasma [3, 4], an electron cyclotron resonance (ECR) plasma [5], and a helicon wave plasma [6]. In particular, it was recently suggested that helicon wave plasmas are accelerated at a large potential drop due to current-free double layer in open field lines. On the other hand, plasma acceleration with applied magnetic field is complex, particularly along the diverging field, and has not been understood well. Hence, it is important to investigate the mechanism of plasma acceleration along open field lines.

For the researches of nuclear fusion, the formation of electric field along open field lines is important. Concerning thermonuclear fusion engineering in a magnetic confinement plasma reactor, the electric potential induced along the open magnetic field has been a crucial topic to improve the confinement characteristics of mirror devices as well as divertor regions of helical or tokamak

reactors [7]. Therefore, it is important to find out the mechanism of potential formation along open field lines.

In this study, we experimentally measure the axial characteristics of cold helium arc jet plasma with an electron temperature of less than 1 eV along open field lines. The helium plasma is generated by arc discharge at near atmospheric pressure. There are a small number of studies on low-temperature plasma characteristics along open field lines. First, we will experimentally confirm that helium arc jet plasma is accelerated. Next, we discuss the mechanism of plasma acceleration and plasma characteristics. We propose a quasi one-dimensional flow model that includes the acceleration both by the increasing cross sectional area of the flow and by the electrical field, and compare the numerical results with the experimental ones.

## 2. Experimental Setup

Figure 1 is a schematic diagram of the experimental setup. Our experimental equipment consists of a rarefied gas wind tunnel, a pumping system, a plasma generator, six electromagnets, a traversing mechanism and a Mach probe.

The rarefied gas wind tunnel had an internal diameter of 1.2 meter and was 2.0 meter long. It was evacuated by the pumping system, which had two 20-inch oil diffusion ejector pumps followed by an 8-inch mechanical booster pump and a 12-inch oil rotary pump. Its pumping speed was about  $10^4$  l/sec. Ultimate pressure was the order of

$10^{-4}$  Torr. During the stationary arc jet expansion, the background pressure was kept at least in the order of  $10^{-3}$  Torr constantly.

Figure 2 shows the schematic diagram of the plasma generator and the electromagnets. An arc discharge is generated between the cathode and the anode in the discharge chamber at near atmospheric pressure. The typical discharge conditions are: a DC arc current of 120 A and a DC arc voltage of about 25 V; the feeding gas is helium (99.5 % pure), and the helium flow rate is about 2.7 mg/s. Electrodes are assembled like a general DC arc torch in the plasma generator [8]. The cathode is made of thoriated tungsten of 3.0 mm in diameter. The anode is made of copper with a 1.2 mm nozzle. Both the cathode and the anode are cooled by water to avoid thermal damage during the plasma discharge. The gap length of the electrodes is controlled by a pulse motor connected to the cathode. The plasma leaves the discharge chamber to the low pressure domain through the anode-nozzle continuously and stably where it is confined by the magnetic field. The magnetic field is generated by the six hollow electromagnets, placed coaxially to the electrode. Each electromagnet has an inner diameter of 80 mm and a thickness of 60 mm. The maximum strength of the

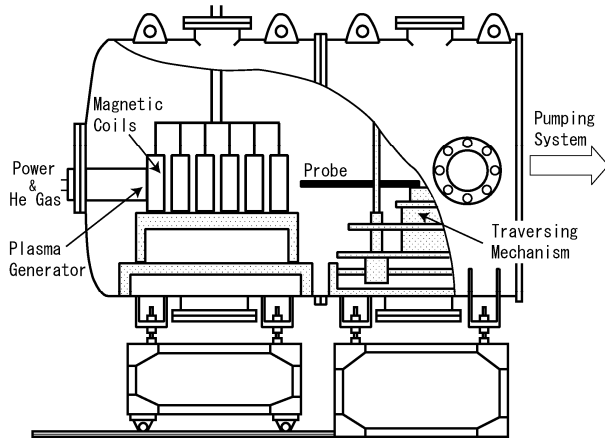


Fig. 1. Schematic diagram of the experimental setup.

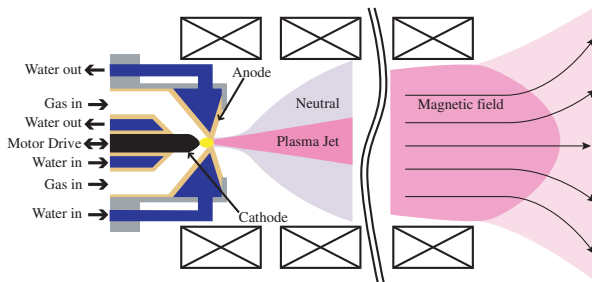


Fig. 2. Schematic diagram of the plasma generator and the magnets.

magnetic field is 0.16 T with a DC current of 300 A. At the end of the electromagnets, open field lines are formed and the plasma is accelerated.

We use a four-tip Mach probe to measure a two dimensional plasma flow structure. The Mach number and the flow direction are measured with a four-tip probe, whose tips face at each side of the square. According to [9], the angle of plasma flow with respect to the probe axis  $\varphi$  and the ion Mach number  $M_i$  are determined from the ratio of each electrode ion saturation currents of each electrode as follows:

$$\varphi = \arctan \left( \frac{\ln \left( \frac{J_D}{J_C} \right)}{\ln \left( \frac{J_A}{J_B} \right)} \right), \quad (1)$$

$$M_i = \frac{M_c}{\cos \varphi} \ln \left( \frac{J_A}{J_B} \right). \quad (2)$$

This probe is moved forward and backward by the traversing mechanism without disrupting the vacuum or interrupting the discharge.

### 3. Results and Discussion

Figure 3 (a)-(e) are the axial profiles of the magnetic field measured by a hole-probe, the axial ion Mach number, the electron temperature, the axial ion velocity and the electron density, respectively. The ion Mach number, the electron temperature, the ion velocity and the electron density are radially integrated. The end of the electromagnets is assigned to the  $z = 0$  mm position. Figure 3 (a) shows that the magnetic field becomes weak at the end of the magnets. From Fig. 3 (b), it is found that the axial ion Mach number increases along open field lines until about  $z = 10$  mm. Hence, it is confirmed that ions are accelerated along the open field lines. The Mach number should be compared with another measurement, such as a Doppler spectroscopy, in order to calibrate the coefficient  $M_c$  in eq. (2). In this study, the Mach number is normalized, so that  $M_i = 1$  in the uniform magnetic field, as it has been already measured by Inutake *et al.* [10]. Figure 3 (c) shows that the electron temperature decreases and is very low, less than 1 eV. The ion velocity is calculated as  $v_i = M_i \times c_s$ , where the sonic velocity of plasma  $c_s = \{k (\gamma_e T_e + \gamma_i T_i) / m_i\}^{1/2}$ , where  $k$ ,  $\gamma_e$ ,  $\gamma_i$ ,  $T_e$ ,  $T_i$  and  $m_i$  are the Boltzmann constant, the electron and the ion polytropic index, the electron and the ion temperature and the ion mass, respectively. Figure 3 (d) shows that the axial ion velocity is accelerated until  $z = 10$  mm, then decreases as well as the ion Mach number. Figure 3 (e) shows that the electron density decreases.

Table 1 shows the collision frequencies and Hall parameters. It is found that ion-electron collision frequency  $\nu_{ie}$ , which is the Coulomb collision between charged particles, is larger than other collisions with neutral particles. Therefore, Hall parameters are calculated by using the coulomb collision frequency. It is also found

that Hall parameters are less than unity for the ion, while larger than unity for the electron. Consequently, the ions are not magnetized, but the electrons are well magnetized. Since the electrons are well magnetized, they are considered to move along the open field lines. Ions are not well magnetized, but they cannot move freely away from electrons due to Coulomb force. As a result, it is considered that the ions also follow the open field lines approximately.

Figure 4 is the vector diagram of the magnetic field calculated for solenoidal electromagnets. The end of the electromagnets is assigned to the  $z = 0$  mm position. It is found that the open field lines are formed at the end of the electromagnets.

Figure 5 shows the vector diagram of the ion flow experimentally measured by the four-tip Mach probe. As it is expected, there is little radial flow component at the center of electromagnets,  $r = 0$  mm. Therefore, it is confirmed that the correct flow direction of the plasma flow can be measured by a four-tip Mach probe. It is also found that the ion Mach number increases at each radial position.

Next, we discuss the mechanism of the ion acceleration. Generally, it is a complex phenomenon because ions are accelerated by aerodynamic and electromagnetic effects, such as a Hall and a swirl effects, and electric field. Figure 6 shows the azimuthal Mach number at each radial position in the electromagnets with the axial position  $z = -40$  mm. It is found that the azimuthal Mach number is small at each radial position. Therefore, it is confirmed that the ions do not rotate in the electromagnets. Consequently, it is concluded that the Hall and the swirl acceleration do not occur. We consider ions are accelerated by the aerodynamic effect and by the electric field. The aerodynamic acceleration is occurred in a supersonic flow, that is Mach number  $M \geq 1$ , when the cross sectional area of the flowing channel increases. We expect the cross sectional area of plasma flowing channel is determined by the magnetic flux conservation. Therefore, we must examine the relationship between the ion flow and the magnetic field.

Figure 7 shows the direction of the ion flow and the magnetic field at the open field lines. It is found that the direction of the ion flow corresponds to that of the magnetic field. Therefore, it is considered that the ions move along the open field lines. As a result, the cross sectional area  $A(z)$  of the plasma flow, which varies with the axial position  $z$ , is determined by the magnetic flux conservation ( $B(z)A(z) = \text{Const.}$ ), where  $B(z)$  is an axial component of the magnetic field.

Then, we consider the electric field. Figure 8 shows the plasma potential distribution. It is found that the plasma potential decreases at each radial position along open field lines. In particular, the largest potential drop is observed at the center of magnets,  $r = 0$  mm. Consequently, it is

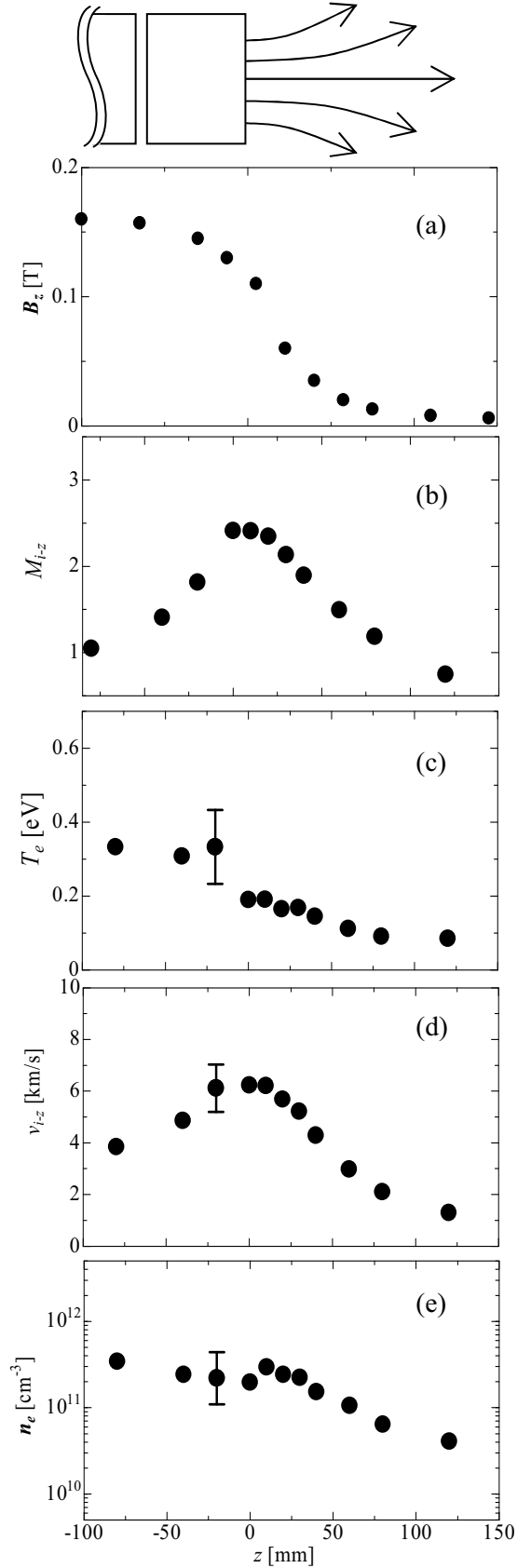


Fig. 3. (a) The axial profiles of the magnetic field, (b) the axial ion Mach number, (c) the electron temperature, (d) the axial ion velocity and (e) the electron density.

Table 1. The collision frequencies between electron-ion  $\nu_{ie}$ , electron-atom  $\nu_{ea}$  and ion-atom  $\nu_{ia}$ , and Hall parameters

$z$ [mm]	$B_z$ [T]	$\nu_{ie}$ [Hz]	$\nu_{ea}$ [Hz]	$\nu_{ia}$ [Hz]	$\beta_i$	$\beta_e$
-40	0.15	$1.6 \times 10^7$	$1.2 \times 10^6$	$1.8 \times 10^3$	$2.3 \times 10^{-1}$	$1.7 \times 10^3$
0	0.11	$5.6 \times 10^6$	$8.8 \times 10^5$	$2.4 \times 10^3$	$4.7 \times 10^{-1}$	$3.4 \times 10^3$
40	0.03	$2.4 \times 10^6$	$7.8 \times 10^5$	$2.7 \times 10^3$	$2.8 \times 10^{-1}$	$2.1 \times 10^3$

confirmed that ions are accelerated by the potential drop.

Finally, let us consider the governing equations. We treat a quasi-neutral and thermodynamic equilibrium plasma through a channel with a cross sectional area  $A(z)$ . In a steady state, the ion continuity equation reduces to the quasi one-dimensional equation

$$\frac{d}{dz}(n_i v_i A) = 0, \quad (3)$$

where  $n_i$ ,  $n_e$  and  $v_i$  are the ion density, the electron density and the ion velocity, respectively.

The ion momentum equation is

$$m_i n_i v_i \frac{dv_i}{dz} = -\frac{dP_i}{dz} - n_i q \frac{d\Phi}{dz}, \quad (4)$$

where  $m_i$ ,  $P_i$ ,  $\Phi$  and  $q$  are the ion mass, the ion pressure, the electric potential and the ion charge, respectively.

To simplify the analysis of temperature variation, we use a polytropic law,  $T_0/T_i = (n_0/n_i)^{\gamma-1}$ , instead of an ion energy equation. The ion pressure using a polytropic law and equation of state (EOS)  $P_i = n_i k T_i$  is

$$\frac{dP_i}{dz} = \gamma k T_i \frac{dn_i}{dz}. \quad (5)$$

Since helium is a monatomic molecule, the polytropic index is assumed to be  $\gamma=5/3$ .

For simplicity, we use the Boltzmann law for the electron density distribution. Therefore, under a quasi-neutral condition  $n_e = n_i$  and thermodynamic equilibrium state  $T_e = T_i$ , the electric field using EOS  $P_e = n_e k T_e$  is

$$\frac{d\Phi}{dz} = \frac{1}{en_i} \frac{d(n_i k T_i)}{dz}, \quad (6)$$

where  $e$  is the elementary charge.

Figure 9 shows the axial profile of the ion Mach number. The solid line represents the numerical results of our model and the filled circles the measured values. Our model closely predicts the axial profile of the ion Mach number in the acceleration zone along the open field lines. Therefore, it is concluded that the helium ions are accelerated both by the electric field and by the increasing cross sectional area of the flowing channel, which is aerodynamic acceleration. Mach number does not agree with the theoretical prediction in the region of  $z > 10$  mm. This phenomenon is caused by collision with neutral particle, which has been already reported by Inutake *et al.* [10]. The charge exchange collisions between the fast ions and atoms are important in the downstream region. To understand the ion deceleration, numerical calculation,

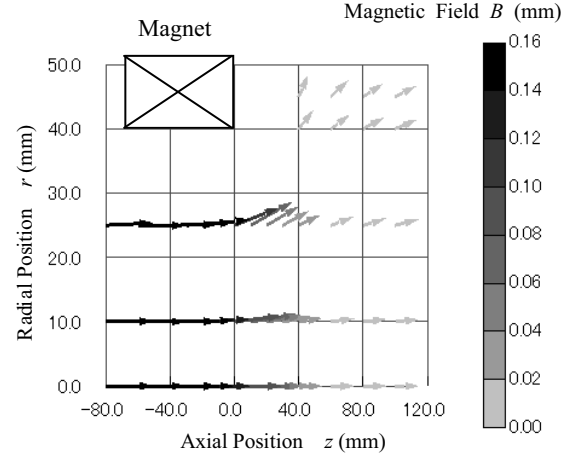


Fig. 4. The vector diagram of the magnetic field calculated for solenoidal electromagnet. (The direction of the magnetic field is conserved with respect to the axis)

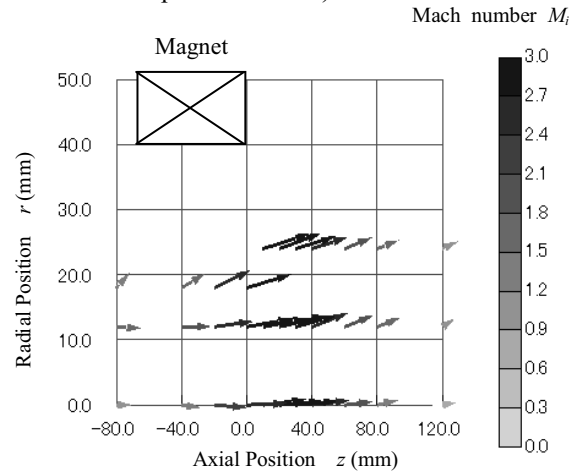


Fig. 5. The vector diagram of the ions flow. (The direction of the ion flow is conserved with respect to the axis)

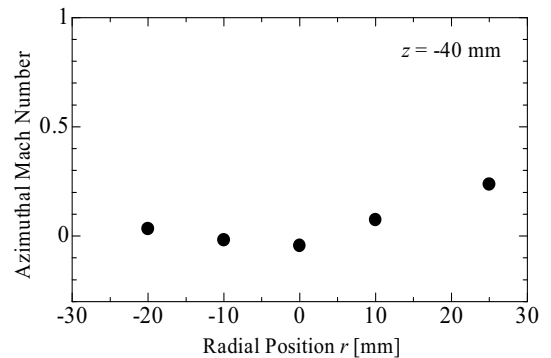


Fig. 6. The azimuthal ion Mach number at each radial position in magnets.

where the rarefied flow effect is also considered, should be carried out because the mean free path is rather long and the Knudsen number  $K_n \approx 0.1$ .

#### 4. Conclusion

We measured the ion Mach number and the plasma potential of helium plasma expanding along open field lines by means of a four-type Mach probe. It was experimentally confirmed that the ions are accelerated along the open field lines. We discuss the mechanism of the ion acceleration. First, the azimuthal Mach number in electromagnets is measured to clarify the contribution of the Hall and the swirl effects to the ion acceleration. The ions do not rotate in electromagnets. Consequently, it is concluded that the Hall and the swirl acceleration do not occur. Next, we investigate the direction of the ion flow and the magnetic field. It is found that the direction of the ion flow corresponds to that of the magnetic field. Therefore, the cross sectional area of the plasma flowing channel is determined by the magnetic flux conservation. Finally, the mechanism of ion acceleration was explained by a quasi one-dimensional flow model including the aerodynamic effect and the electric field, in which plasma is assumed to be quasi-neutral and in a state of thermodynamic equilibrium. Therefore, it is concluded that the helium ions are accelerated both by the electric field and by the increasing cross sectional area of the flowing channel, which is determined by the magnetic flux conservation ( $B(z)A(z) = \text{Const.}$ ).

#### 5. References

- [1] A. Kanzawa, *Plasma heat transfer*, (Shinzan Press, Tokyo, 1992) p.24 (in Japanese).
- [2] I. G. Brown, *Rev. Sci. Instrum.* **65**, pp.3061–3081 (1994).
- [3] H. Nishiyama, T. Saisu, M. Okubo and S. Kamiyama, *Trans. JSME. Ser. B.* **59**, pp.1854–1862 (1993).
- [4] M Keidar, I Beilis, R L Boxman and S Goldsmith, *J. Phys. D: Appl. Phys.* **29**, pp.1973–1983 (1996).
- [5] W. M. Manheimer and R. F. Fernsler, *IEEE Trans. Plasma Sci.* **29**, pp.75–84 (2001).
- [6] C. Charles and R. Boswell, *Appl. Phys. Lett.* **82**, pp.1356–1358 (2003).
- [7] K. Sato, *J. Plasma Fusion Res.* **68**, pp.562–567 (1992).
- [8] H. Akatsuka and M. Suzuki, *Rev. Sci. Instrum.* **64**, pp.1734–1739 (1993).
- [9] A. Ando and S. Kado, *J. Plasma Fusion Res.* **83**, pp.167–175 (2007).
- [10] M. Inutake, A. Ando, K. Hattori, H. Tobari, and T. Yagai, *J. Plasma Fusion Res.* **78**, pp.1352–1360 (2002).

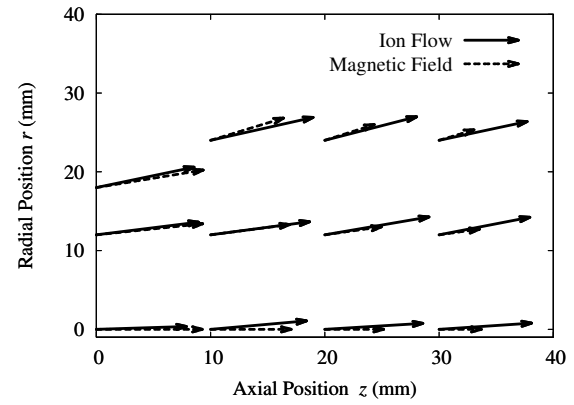


Fig. 7. The vector diagram of the ion flow and the magnetic field. (The directions of the magnetic field and the ion flow are conserved with respect to the axis)

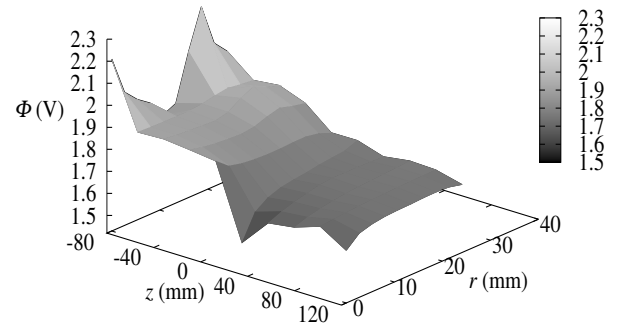


Fig. 8. The plasma potential distribution.

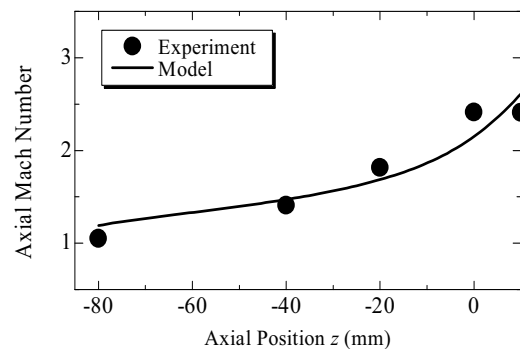


Fig. 9. The axial profiles of the axial ion Mach number.